Sub-axial deformation in oceanic lower crust: Insights from seismic reflection profiles in the Enderby Basin and comparison with the Oman ophiolite

Daniel Sauter, Philippe Werner, Georges Ceuleneer, Gianreto Manatschal, Mathieu Rospabé, Julie Tugend, Morgane Gillard, Julia Autin, Marc Ulrich

Sub-axial deformation in oceanic lower crust: insights from seismic reflection profiles in the Enderby Basin and comparison with the Oman ophiolite.

Daniel Sauter[1], Philippe Werner[1], Georges Ceuleneer[2], Gianreto Manatschal[1], Mathieu Rospabé[3], Julie Tugend[4], Morgane Gillard[4], Julia Autin[1] and Marc Ulrich[1]

(1) Institut de Physique du Globe de Strasbourg (IPGS), UMR7516 CNRS Université de Strasbourg, 1 rue Blessig, 67084 Strasbourg Cedex, France ; corresponding author : daniel.sauter@unistra.fr
(2) Géosciences Environnement Toulouse (GET), Observatoire Midi Pyrénées, Université de Toulouse, CNRS, IRD, 14 avenue E. Belin, 31400 Toulouse, France
(3) Research Institute for Marine Geodynamics (IMG), Japan Agency for Marine-Earth Science and Technology (JAMSTEC), 2-15 Natsushima, Yokosuka, Kanagawa 237-0061, Japan
(4) Institut des Sciences de la Terre Paris (ISTeP), UMR 7193, Sorbonne Université, CNRS, 4 Place Jussieu, 75005 Paris, France

Reference to cite:
Sauter, D., Werner, P., Ceuleneer, G., Manatschal, G., Rospabé, M., Tugend, J., Gillard, M., Autin, J., and Ulrich, M., 2021, Sub-axial deformation in oceanic lower crust: Insights from seismic reflection profiles in the Enderby Basin and comparison with the Oman ophiolite: Earth and Planetary Science Letters, v. 554, p. 116698, doi:https://doi.org/10.1016/j.epsl.2020.116698.

Abstract

We analyzed high-quality seismic reflection profiles across the ocean-continent transition in the Enderby Basin between the Kerguelen Plateau and the Antarctic margin. There, we observe numerous high-amplitude dipping reflections in the lower oceanic crust which was accreted at a magmatic spreading center as testified by the almost uniform 6.4-7 km thick crust and its unfaulted, flat top basement. The deep reflections are rooting onto the Moho and are dipping both ridgeward and continentward. They occur in dense networks in mature oceanic crust as well as close to the continentward termination of oceanic crust and in the ocean-continent transition zone. The comparison with field observations in the Oman ophiolite suggests that these lower crustal dipping reflectors could correspond to syn-magmatic faults. In Oman, very high temperature (up to syn-magmatic), high temperature (sub-solidus plastic deformation) and low temperature (brittle) deformation coexist along the same fault over distances of a few hundred meters at Moho level. This very high temperature gradient may be explained by the sudden and intense interaction between crystallizing magmas and hydrothermal fluids induced by the episodic nucleation of faults in a context of continuous magmatic spreading. The igneous layering becomes extremely irregular compared to its monotonous sub-horizontal orientation away from the faults which, together with enhanced hydrothermal alteration restricted to the fault zones, might change the physical properties (velocity, density) and increase the reflectivity of syn-magmatic faults. We further speculate that these processes could explain the brightness of the lower crustal dipping reflectors observed in our seismic reflection data. Both the seismic reflection profiles of the Enderby Basin and the Oman ophiolite show evidence for syn-accretion tectonism at depth together with the systematic rotation of originally horizontal lava flows or originally vertical dikes, pre-dating cessation of magmatic activity. This indicates ubiquitous deformation processes within the axial zone of magmatic spreading centers.

Keywords

Lower oceanic crust; oceanic accretionary processes; dipping reflectors; ocean-continent transition; Enderby Basin; Oman ophiolite.

1. Introduction

Most of the oceanic crust created over the last 200 million years formed at intermediate- to fast-spreading mid-ocean ridges (50-200 km/Ma full rate) (Karson, 2002). Despite the widespread occurrence of such magmatic crust, direct observations of its lower part made essentially of gabbroic cumulates are particularly scarce. There are only two locations (Hess Deep and Pito Deep in the Pacific Ocean) where *in situ* fast-spread plutonic crust is exposed in response to ridge propagation. Rocks from such deep horizons have been collected by submersible, remotely operated underwater vehicle and drilling, the section recovered by drilling being typically several tens of meter in length only (e.g. Brown et al., 2019; Gillis et al., 2014). No *in situ* observations within the lowermost oceanic crust accreted at fast-spreading ridges have been made elsewhere, apart from some sites in large offset transform faults, where crustal structures might not be representative of standard accretion processes (cf. Constantin et al., 1996).

Therefore, our knowledge of the deep crustal magmatic system along fast-spreading mid-oceanic ridges is mostly derived from seismic studies of the East Pacific Rise (EPR) and ancient analogues (e.g. ophiolites) although the tectonic setting of their genesis is still debated (MacLeod et al., 2013). Seismic reflection data have shown that there is a near static region of high melt proportions, the axial magma lens (AML), 1-3 km wide and a few hundred meters high, at a depth of 1-2 km beneath the ridge axis, for much of its length (e.g. Detrick et al., 1987). Beneath the AML, tomographic studies have indicated that there is a low velocity zone a few kilometers wide (e.g. Toomey et al., 1990), which is inferred to consist of a crystal mush, i.e. incompletely crystallized cumulates (Sinton and Dietrick, 1992). More recent seismic reflection studies have shown a series of melt lenses in the lower crust below the AML both on and off-axis (e.g. Marjanovic et al., 2014). In addition, melt in the lower crust and/or the crust-mantle transition zone was also inferred by seafloor compliance studies (Crawford and Webb, 2002). Thus, there is an increasing set of arguments for a multi-level complex of melt lenses beneath the ridge axis (Marjanovic et al., 2014).

However, how these melt lenses contribute to the formation of both the upper and lower crust and what accretion processes are operating in the lower crust remain unclear. Two end-member models for crustal accretion have emerged from geophysical observations at fast-spreading ridges and more largely from field evidence in the Oman and other ophiolites (Kelemen et al., 1997; Marjanovic et al., 2014; Nicolas and Boudier, 2015). In the `gabbro glacier' model, most crystal growth occurs within the AML, which subsides by ductile flow to form the entire gabbro section (e.g. Quick and Delinger, 1993). The `sheeted sill' model, where gabbro formation occurs *in situ* in small magma bodies throughout the lower oceanic crust, better fits with the occurrence and structure of the interlayered mafic and ultramafic cumulates in ophiolites (Kelemen et al., 1997). In the Oman ophiolite, recent studies of the crust-mantle transition zone have shown that faults, enabling water introduction at depth, may be a more common feature than previously expected in the formation of the lowermost oceanic crust in a

context of high melt supply (Abily et al., 2011; Rospabé et al., 2019). Such faults have not been documented yet in seismic reflection profiles at fast-spreading ridges. However, lower crustal dipping reflectors have been observed on ridge flanks within both slow- and fast-spreading crust (see Bécel et al. (2015) for a review) while they are not imaged along the ridge axis itself. Such lower crustal dipping reflections within fast-spread crust have been interpreted as arising from shear zones that form near the spreading center in the region with interstitial melt, and result from shear at the base of the crust (Bécel et al., 2015). It has been further suggested that such differential motion at the base of the crust could result from plate reorganizations (Bécel et al., 2015).

While lower crustal events dipping toward the paleo-ridge axis have been predominantly described until now (Bécel et al., 2015; Ding et al., 2018; Reston et al., 1999), here we identify numerous both ridgeward and continentward dipping high-amplitude reflectors in the lower oceanic crust of the Enderby Basin, between the Kerguelen Plateau and the Antarctic margin. Thanks to high-quality seismic reflection profiles, we are able to document the occurrence of such dipping reflections in two different but juxtaposed domains: typical oceanic crust and the ocean-continent transition. We relate these lower crustal dipping reflectors to syn-magmatic faulting described recently in the Oman ophiolite (Abily et al., 2011; Rospabé et al., 2019). These observations give some clues for the sub-axial tectono-magmatic processes that may occur within the oceanic crust.

2. Geological background

2.1. The Enderby Basin

Here, we focus on the oceanic domain and the ocean-continent transition within the central part of the Enderby Basin. It is bounded by the Enderby Land to the southwest, by the Elan Bank to the north and the southern Kerguelen Plateau to the northeast, by the Princess Elizabeth Trough to the east and by the Antarctic margin and the Mac Robertson Land to the south (Fig. 1). The Enderby Basin is thought to be formed during the Early Cretaceous as East Antarctica and India rifted apart (McElhinny, 1970). An intermediate spreading rate of ~60 km/Ma has been inferred from east-west trending magnetic anomalies M4 (126.7 Ma), M2 (124.1 Ma), and M0 (120.4 Ma) (Gibbons et al., 2013). These anomalies have been identified north and south of an extinct ridge running parallel to the Elan Bank (Gaina et al., 2007) (Fig. 1). However, this extinct ridge is poorly constrained and, contrasting with many other extinct ridges, it is not linked to a gravity low (MacLeod et al., 2017). Moreover, magnetic anomaly profiles in the Enderby Basin are scarce and, due to the absence of clear and continuous magnetic anomalies, their identification is debated (e.g. Golynsky et al., 2013). It has been suggested that the lack of clear magnetic anomalies may result from seafloor spreading during the Cretaceous Normal Superchron (Jokat et al., 2010). Therefore, no consensus about the spreading history of the Enderby Basin has been reached yet (e.g. Davis et al., 2018).

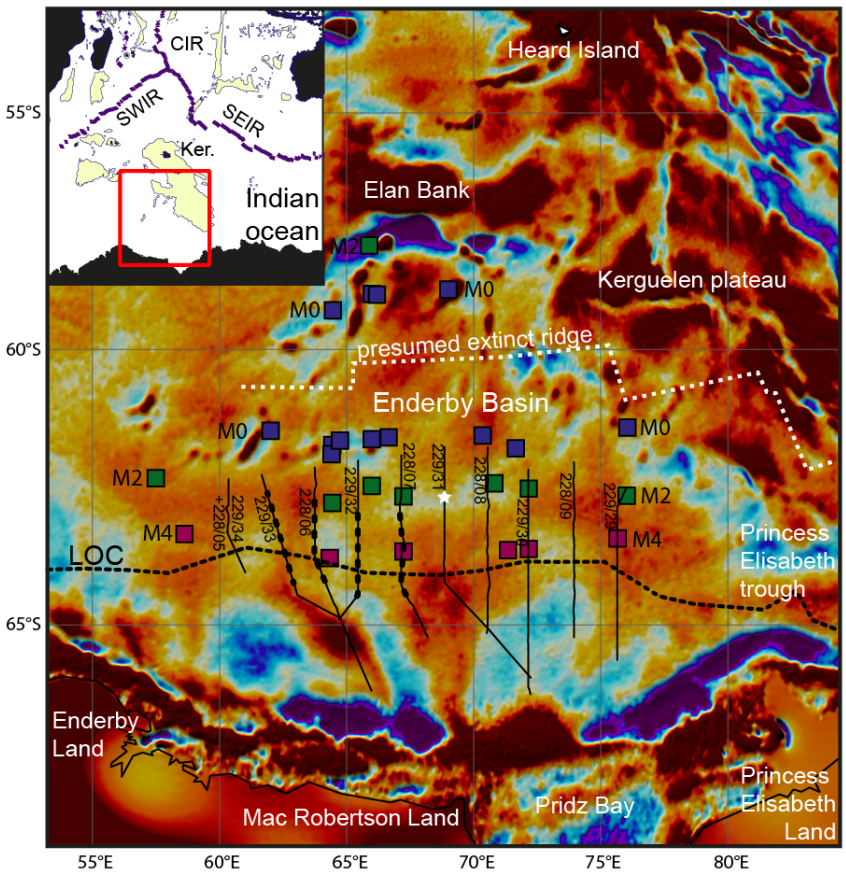

Fig. 1: Map of the eastern Enderby Basin. The background image is the free air gravity anomaly grid derived from satellite altimetry data (Sandwell et al., 2014). The black dashed line indicates the landward edge of the oceanic crust (LOC) after Gaina et al. (2007). The white dashed line indicates the presumed extinct ridge axis after Gibbons et al. (2013). The squares show the magnetic anomaly picks from Gibbons et al. (2013). The black lines indicate the seismic profiles from Geoscience Australia used in this paper. Their thickened and dashed parts correspond to the sections shown in Fig. 3. The white star indicates the location of Fig. 6. Ker., Kerguelen Island; CIR, Central Indian Ridge; SEIR, Southeast Indian Ridge; SWIR, Southwest Indian Ridge.

By contrast, there is a consensus about the location of the inboard edge of unequivocal oceanic crust (LOC) (Fig. 1). It typically coincides with: (1) a prominent oceanward step-up in the basement level of 500-1000 m, (2) the continentward abrupt termination of a well-marked oceanic Moho in the seismic reflection profiles (Stagg et al., 2005), and (3) the Enderby Basin Anomaly (EBA; (Golynsky et al., 2013), a high-amplitude (350–500 nT) magnetic anomaly which is interpreted to mark the contact between strongly magnetized oceanic crust and less magnetized continental rocks (Golynsky et al., 2013). The domain to the north of the LOC is described as unambiguous oceanic crust (Stagg et al., 2005). The domain immediately to the south, within the ocean-continent transition, is referred to as transitional crust on the basis of seismic reflection profiles and limited refraction data (sonobuoys) (Stagg et al., 2005). It is thought to be made of stretched continental crust or exhumed mantle that was subsequently modified by magmatic intrusions during the formation of the initial- or proto-oceanic crust (Gaina et al., 2007; Gillard et al., 2019).

We use 10 high-resolution and deep-penetrating seismic reflection profiles from the GA-228 and GA-229 surveys collected by Geoscience Australia in 2000 and 2001, respectively (Stagg et al., 2005). During these surveys, 36-fold stacked and migrated deep seismic data (60 l airgun array source; 3600 m streamer; 288 channels; 16 s

record length) were recorded between offshore western Enderby Land and the southern Kerguelen Plateau (Fig. 1) (Stagg et al., 2005). The seismic profiles are trending North-South, perpendicular to the LOC and the magnetic lineations of the Enderby Basin. They are thus thought to be collected along a flow line of the Enderby Basin spreading center, although the geometry and segmentation of this ridge is poorly known. This data set was used by Stagg et al. (2005) to map and describe distinct sectors along the Antarctic margin and the adjacent oceanic crust.

2.2. The Oman ophiolite

The Oman ophiolite is the largest coherent remaining fragment of the Tethyan oceanic lithosphere. It is interpreted as formed along a highly productive (Ceuleneer et al., 1996; Pallister and Hopson, 1981) and possibly fast-spreading center ~95-97 million years ago (Boudier et al., 1985; Rioux et al., 2012). Major ductile shear zones were recognized as common features in the mantle and crustal sections of the Oman ophiolite since pioneer structural studies (Amri et al., 1996; Boudier et al., 1985; Boudier et al., 1988; Jousselin and Nicolas, 2000; Jousselin et al., 1998). They are characterized by intense deformation with the development of peridotite mylonites and flaser gabbros on thicknesses ranging from a few meters to several hundred meters. The main ones can be followed along strike over distances of several tens of kilometres. Shearing initiated at very high temperature, close or above the solidus of peridotites and gabbros, frequently in the presence of melt, and usually stopped before the rock cooled down significantly, although most of these shear zones were still active at greenschist facies metamorphic conditions.

The shear zones revealed by the early structural mapping of the Oman ophiolite show a clear continuity with the metamorphic sole and, hence, have been attributed to emplacement tectonics (intra-oceanic thrusting close to the ridge axis) (Boudier et al., 1985; Boudier et al., 1988). Until recently, this interpretation was extended by most geologists to all kinds of ductile and brittle fault zones affecting the mantle and the deep crustal section of the Oman ophiolite, apart from minor ones interpreted in terms of oceanic spreading (e.g. Dijkstra et al., 2002). Circularity in the way of reasoning maintained the confusion: Oman ophiolite being supposed to derive from a fast-spreading centre where faulting (at least down to deep levels of the crust) was supposed to play an anecdotic role relative to igneous accretion, faults observed in Oman were *a priori* attributed to later events, among other the intra-oceanic thrusting. However, more detailed studies have revealed the existence of high temperature shear zones, which did not record strike slip or inverse kinematics calling for convergent tectonics. A normal shear sense is actually recorded by many faults among those which have an azimuth subparallel to the one of paleo-ridge axis, including high temperature ductile faults (Abily et al., 2011; Rospabé et al., 2019).

Moreover, our structural observations and petrological data from the Maqsad area highlight that faults were active early at Moho level, since the magmatic stage, and that they contributed to the petrological and geochemical organization of the lower crust. Due to the deep introduction of water they triggered, these faults exerted a strong control on the reaction leading to the transformation of mantle harzburgite into dunite at the Moho and on melts migration and crystallization paths, and continued to serve as major avenues for hydrothermal fluids down to lower temperatures (Abily et al., 2011; Rospabé et al., 2017). These faults are either parallel to the strike of the sheeted dike complex (*i.e.* parallel to the regional orientation of the inferred paleo-ridge axis) or

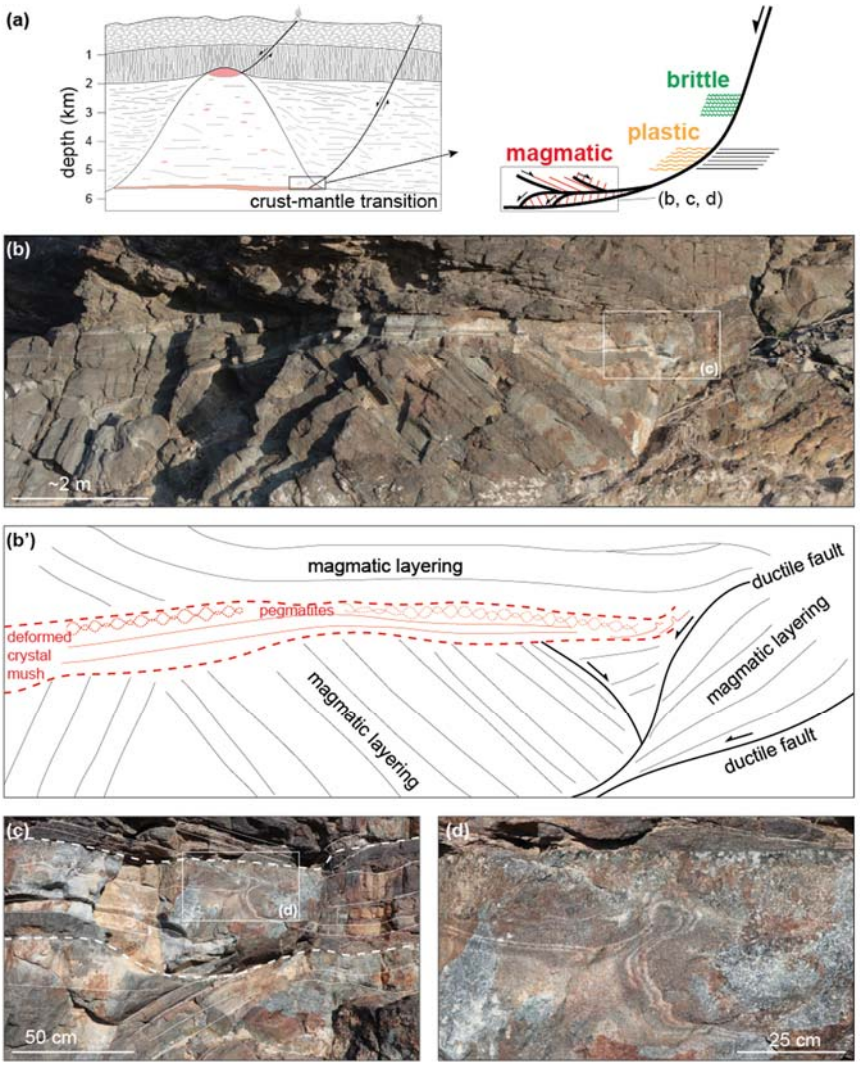

Fig. 2: Evidence of syn-magmatic normal faulting and block rotation at Moho level in the Oman ophiolite, Maqsad area (see also Abily et al. (2011)). (a) Simplistic sketches illustrating the possible context of acquisition of the structures observed in the field (left) and the evolution in the conditions of deformation along the fault (right). (b) Main structural elements observed on this outcrop: magmatic layering (thin black lines); ductile faults (thick black lines and arrows), deformed crystal mush layer (red symbols). (c) Closer view on the zone of former crystal mush with complex modal layering induced by crystal sorting and melt injection during viscous deformation. (d) Detail on a ptygmatic fold and on the upper horizon of pegmatite (former melt layer that made possible the mechanical decoupling between the tilted blocks of layered cumulates and the overlying cumulates).

slightly oblique to it (Rospabé et al., 2019). They mostly have a ridgeward dip ranging from 65° to 10° and some are clearly listric, with dips progressively shallowing as the crust-mantle boundary is approached, inducing early tilting of blocks of hardly consolidated layered cumulates (Fig. 2). Normal syn-accretion faults highly altered in a wide temperature range have been identified in other massifs of the Oman ophiolite (e.g. Zihlmann et al., 2018) and seem to be the rule rather than the exception. In the case of the fault studied in detail by Abily et al. (2011), the rotation of these blocks of layered cumulates, at high angles relative to the Moho, was accommodated by an anastomosing fault network connected to the main fault plane. It is locally underlined by thin screens of gabbroic micropegmatites, which represent former hydrated evolved melts crystallizing as amphibole-bearing gabbros and by ptygmatic folds, pointing to viscous deformation of a sheared and compacting crystal mush (Abily et al., 2011) (Fig. 2). Flat-lying undeformed cumulate layers, in the same differentiation stage as

the deformed ones, settled directly over the tilted blocks, which is the main evidence for syn-magmatic block rotation (Fig. 2). In this example, outcrops witnessing syn-magmatic deformation exceptionally escaped lower temperature deformation and alteration. This evidences a remarkable lateral evolution in the deformation style on a distance of a few hundred meters. Moving away from the zone where syn-magmatic structures are preserved, i.e. moving toward the main fault that was active down to greenschist facies conditions, shearing continued at sub-solidus temperatures along some fault planes, and brittle deformation structures become more and more prevalent (Abily et al., 2011).

Lower crustal gabbros from Oman generally present a quite regular igneous (modal) layering sub-parallel to the crust-mantle boundary ("paleo-Moho"). This monotonous orientation is totally disturbed within several hundred meters from these syn-magmatic normal faults. Minor faults are spaced by a characteristic distance of ~250 m on average, but the major ones may be several kilometers apart. Moving from the top to the base of the crust-mantle transition zone, the deformation conditions evolved from brittle to ductile. Most of these faults were active in a broad temperature interval, with the development of serpentine and carbonate breccias that can be intruded by gabbroic dikes altered in greenschist facies conditions. These brecciated zones reach up to 10 m in thickness in the few major faults and have been zones of intense fluid circulation (Rospabé et al., 2019). The fact that water penetration occurred early during the development of these faults is attested by geochemical gradients continuous on distances reaching a few dozen of meters away from the faults (Rospabé et al., 2019). Concerning the lower temperature water circulation and greenschist facies alteration, the connection with former seafloor hydrothermal vents is attested by the occurrence of Fe, Ni and Cu sulfide mineralizations within these faults (Abily et al., 2011).

A recent survey showed that the Moho steepens in the massifs located close to the front of the Oman ophiolite. This unusual dipping is attributed to a ductile shear zone that was active in very high temperature conditions, close to the gabbro solidus (Ceuleneer et al., 2020). The lower crustal cumulates are affected by plastic deformation on a thickness reaching 2 km and the along strike extent of the fault reaches 100 km subparallel to the paleo-ridge axis. The curvature of this mega-fault was continentward at the time of accretion. Away from the Moho, the decrease in the deformation intensity is correlated with a progressive flattening of the layering and foliation of the gabbros (listric fault kinematics). This major feature, of regional extent, is interpreted in terms of syn-accretion tectonics (Ceuleneer et al., 2020).

3. Description of the seismic reflection profiles in the Enderby Basin

Here we gather several examples from different seismic profiles to get an all-encompassing view of the typical seismic structures from the unambiguous oceanic crust in the northern part of the survey area to the ocean-continent transition zone to the south.

3.1. The northernmost part of the survey area

In the northernmost end of the seismic sections we observe a well-defined oceanic crust characterized by: (1) a smooth flat and reflective top basement, (2) some short reflections in the shallowest part of the crust, (3) a transparent unit in the upper crust

located above, (4) a more reflective lower crust, and (5) a set of horizontal reflectors at the base of the crust. We interpret this latter as the oceanic Moho, although various geological structures at the base of the crust may generate high-amplitude reflections (e.g. Collins et al., 1986). The thickness of the oceanic crust is usually 2-2.2 s TWTT corresponding to ~6.4-7 km (using Canales et al. (2003) relationship between crustal thickness and crustal reflection travel times), which is within the range of normal oceanic crust thicknesses (6 ± 1 km; e.g. Christeson et al., 2019). In some places the crust is thicker than the normal oceanic crustal thickness. This is the case south of the Kerguelen plateau, where the crustal thickness reaches 3.2 s TWTT (~10 km) but also at the western edge of the survey area where the crust reaches 2.5 s TWTT thickness (7.9 km at 60°E) (Supplementary Fig. S1). Both the flat top basement and the thickness of the oceanic crust argue for a formation at a magma-rich spreading center.

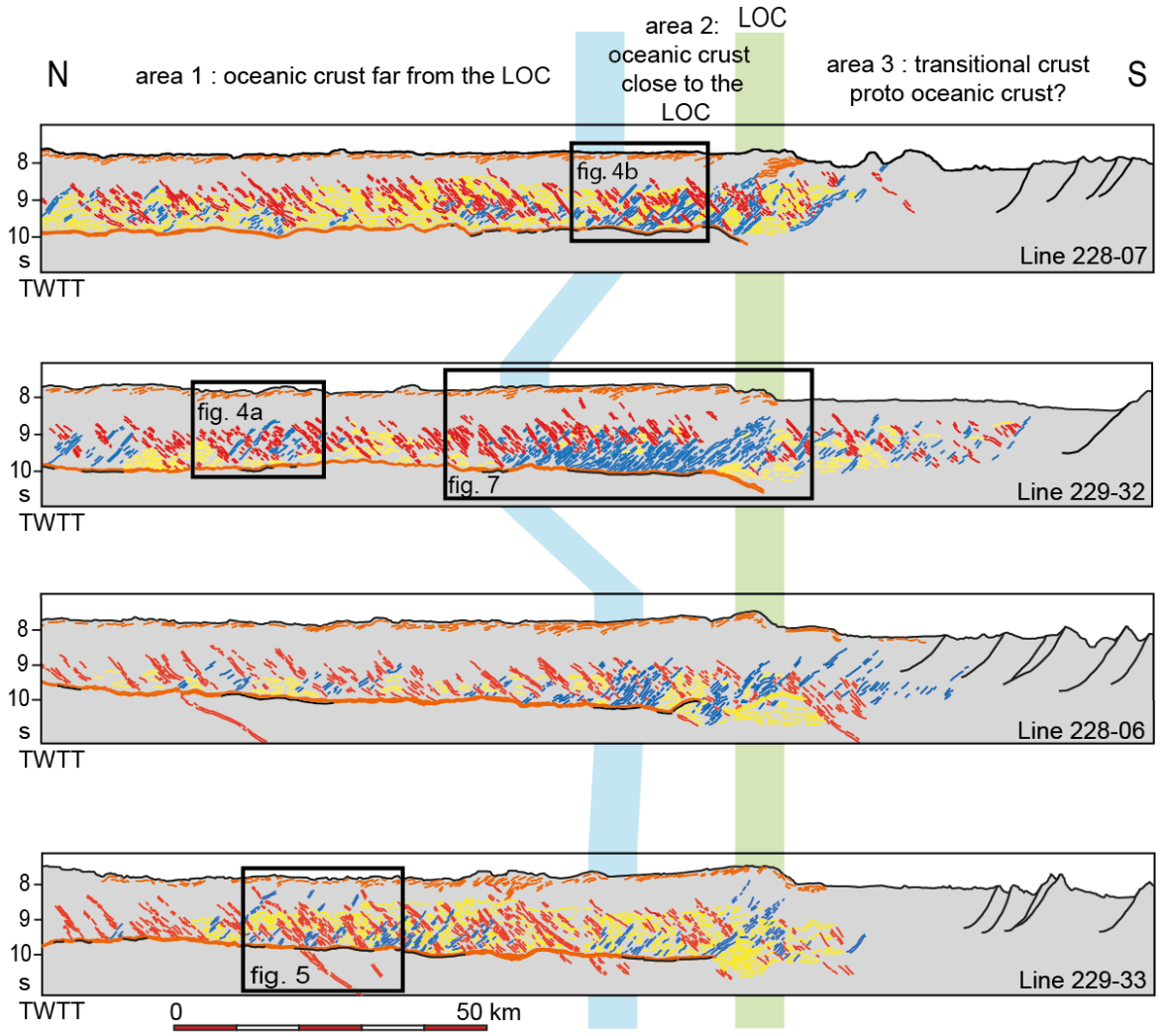

Fig. 3: Line drawing of 4 seismic profiles across the landward edge of the oceanic crust (LOC indicated by the green band). Blue lines indicate oceanward dipping reflectors (ODRs); red ones indicate continentward dipping reflectors (CDRs); yellow ones show nearly horizontal reflectors and orange ones at the top basement indicate oceanic seawards dipping reflectors (OSDRs). The thick orange lines at the bottom of the crust show the reflection Moho and the black lines beneath it show where the Moho is continuous and highly reflective. The blue band indicates the ridgeward end of the dense network of ODRs occurring close to the LOC. Vertical exaggeration is approximately x2. Uninterpreted and interpreted versions of profiles 229/32 with no vertical exaggeration are shown in the Electronic Supplement 1.

3.2. *Oblique reflectors in the oceanic crust away of the LOC (area 1)*

To the south, in area 1 (see Fig. 3), the most striking and intriguing features of the seismic reflection profiles are the numerous high-amplitude dipping reflectors in the lower oceanic crust. These deep reflectors occur along sections more than 150 km-long. They define a layer of almost constant thickness at the base of the oceanic crust (1.3 s TWTT on average that is ~4.6 km using a 7 km/s for the lower crust) (Electronic Supplement 1). A discontinuous upper horizontal reflector marks locally the top of this lower crustal layer (at 0.7-0.8 s TWTT depth below top basement that is ~1.9 km using a 5 km/s for the upper crust). At the base, the reflection Moho is well marked and defines an oceanic crust of normal thickness (~2-2.1 s TWTT on average) (Fig. 3).

The spacing between the deep reflectors is variable, reaching several kilometers. However, in sections where their distribution is more regular, the spacing is typically 2 km. There, they are 5-6 km-long. Locally and rarely, they can reach 10 km-long where they reach the upper crust. While they dip either toward the continent or toward the ridge, they mostly occur as series of reflectors dipping in the same direction for several tens of kilometers before changing dip direction (Fig. 3). Such changes in the dip direction are not marked by any noticeable change neither at the top basement nor at the reflection Moho. Multiple changes of dip direction also occur locally such as in profile GA-229/32, where lower crustal reflectors are crossing each other (Fig. 4a).

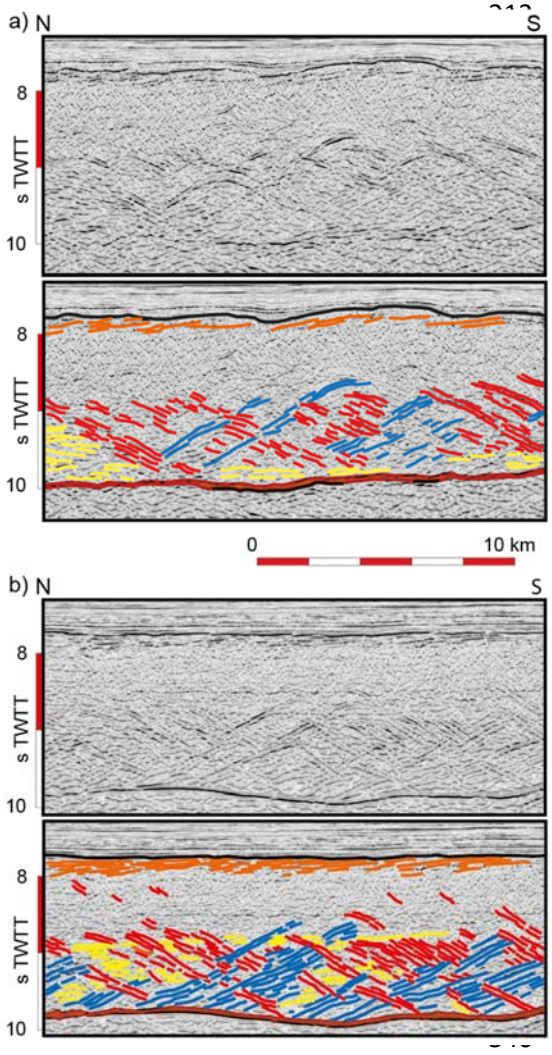

Fig. 4: Examples of dipping reflectors crossing each other (a: profile 229/32 and b: profile 228/07) defining a layer of almost constant thickness at the base of the oceanic crust. The reflection Moho is well marked almost all along the bottom of the layer. See figure caption and location in Fig. 3. Approximately no vertical exaggeration. Copyright Commonwealth of Australia (Geoscience Australia).

The deepest part of the lower crustal reflectors roots at the reflection Moho and their shallowest part flattens at the base of the transparent layer, giving them a general apparent sigmoidal shape (Fig. 4a and S2). Although the exact geometry of the reflectors is unknown (as we do not know the seismic velocity profile) we note that some of these reflectors merge with shallower horizontal ones (Supplementary Fig. S2). Rare deep reflectors are observed both in the crust and in the mantle as deep as 11.5 s TWTT (Fig. 5).

A few rising continentward dipping reflectors (CDRs) are observed in the upper crust but they do not reach the top basement. They are covered by long and continuous reflectors (reaching 4-5 km length), which are ubiquitous in the shallowest part of the crust (Figs. 4 and 5). The thickness of this

set of shallow reflectors is on average 0.5 s TWTT (1 km using a 4 km/s velocity for the uppermost crust) but may reach 0.7-0.8 s TWTT locally (1.5 km at 4 km/s). These shallow reflectors mostly dip gently toward the ridge at the base and then become horizontal upward forming wedges, up to 10 km-long, in the uppermost part of the crust (Fig. 6). Within these wedges, the CDRs that rise up from the lower crust are discontinuous, distributed, short and almost perpendicular (on the time sections) to the shallow reflectors dipping toward the ridge. Because these shallow reflectors remind the seaward dipping reflectors (SDRs) observed at volcanic rifted margins, we have call them oceanic seaward dipping reflectors (OSDRs). Despite the occurrence of these OSDR wedges, the top basement is usually almost flat or very smooth and only very rare volcanoes or faults can be inferred from the seismic reflection of the top basement (Supplementary Fig. S3).

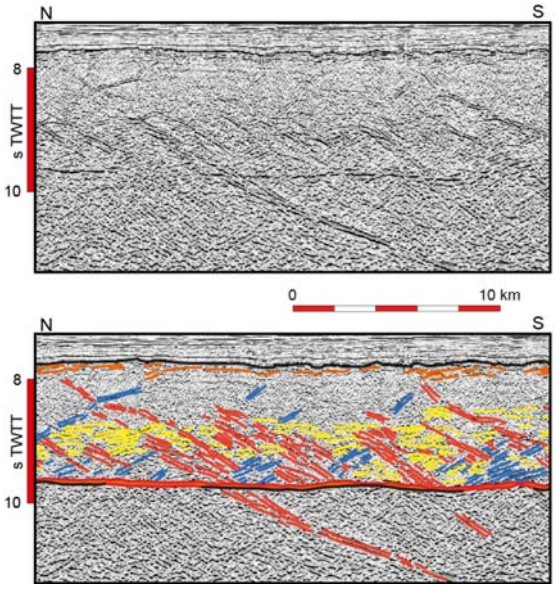

Fig. 5: Example of reflectors that are observed both in the crust and in the mantle as deep as 11.5 s TWTT (line 229/33). Note some rare examples of dipping reflectors that are shallowing but do not reach the top basement as they are covered by long and continuous reflectors. See figure caption and location in Fig. 3. Approximately no vertical exaggeration. Copyright Commonwealth of Australia (Geoscience Australia).

3.3. A specific network of lower crustal dipping reflectors close to the LOC (area 2)

In area 2, close to the LOC (see Fig. 3), some profiles show a 20-40 km-long denser network of deep oceanward dipping reflectors (ODRs; 1 reflector every ~500 m), which systematically sole out onto the reflection Moho. This is particularly well observed in profile GA-229/32 (Figs. 3 and 7). There, a few ODRs reach the upper crust at the LOC and are progressively replaced by CDRs with higher reflectivity (Fig. 7). Short CDRs first observed in the mid-crust close to the LOC where the crust is thicker (2.4-2.8 s TWTT), are lengthening and deepening oceanwards. The CDRs finally reach the reflection Moho as the ODRs disappear at 30-40 km from the LOC.

This dense network of ODRs close to the LOC shows some variability from one profile to the other: e.g. profile GA-228/07 displays triangular-shaped areas with groups of deep reflectors dipping preferentially oceanwards or continentwards (Figs. 3 and 4b). The top basement remains flat in area 2 except in profile GA-229/30. There, it is associated with a wedge of shallow reflectors in the uppermost crust beneath a small asymmetric basin at the seafloor (Supplementary Fig. S4). The ODRs systematically sole out onto the Moho, which is particularly well marked by a single continuous bright reflector (Figs. 3 and 7). In this area the Moho is nearly horizontal or slightly dipping continentwards, defining a thicker oceanic crust (~2.4 s TWTT) than in area 1 (Fig. 7).

384 At the LOC the Moho branches out in a set of deep reflectors that shallow or deepen
385 parallel to the ODRs and CDRs, respectively (Figs. 7 and S5).

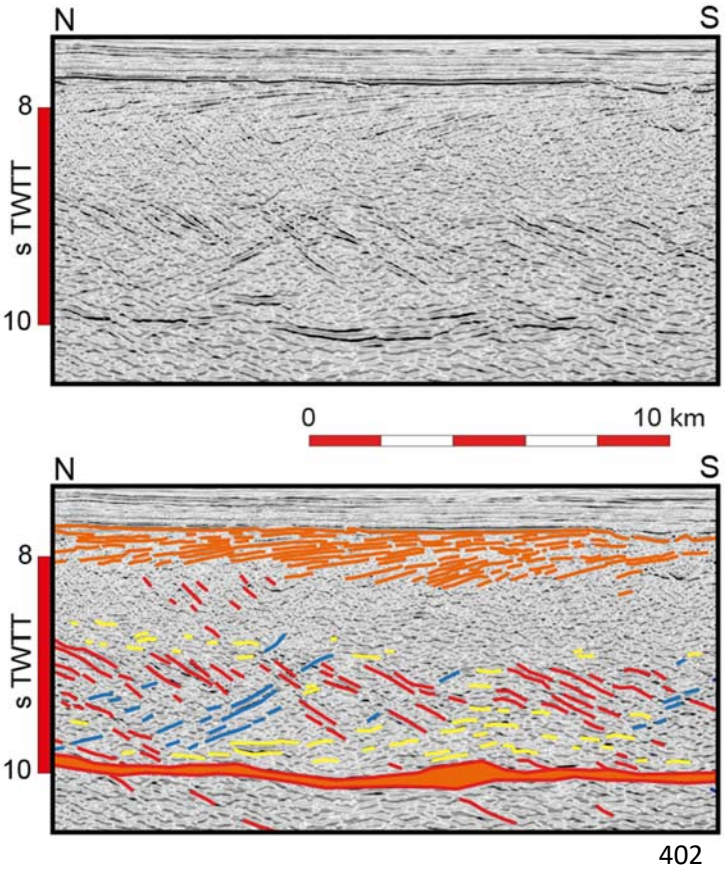

Fig. 6: Example of oceanic seawards dipping reflectors (OSDRs) forming up to ~10 km-long wedges in the uppermost part of the crust (profile 229/31). Same figure caption as Fig. 3. See location in Fig. 1. Approximately no vertical exaggeration. Copyright Commonwealth of Australia (Geoscience Australia).

402

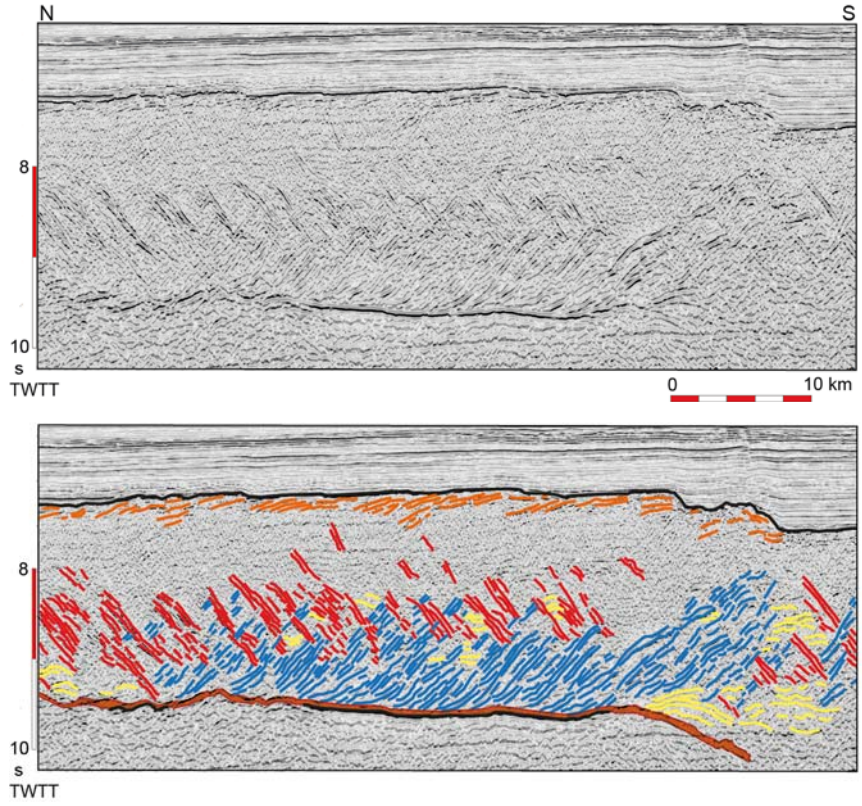

Fig. 7: Denser network of oceanward dipping reflectors (ODRs) and continentward dipping reflectors (CDRs) (1 reflector every ~500 m) close to the landward edge of the oceanic crust (profile 229/32). Vertical exaggeration is approximately 2x. See figure caption and location in Fig. 3. Copyright Commonwealth of Australia (Geoscience Australia).

Above the termination of the reflection Moho, an oceanward step-up in the top basement is systematically observed (Fig. 7). It is 0.5 TWTT high (~1000m at 4 km/s for the uppermost crust) on average. Locally, within this basement high, 2-3 shallow reflectors are slightly dipping oceanwards and are recovered progressively by flatter lying reflectors in a fan shape structure, similarly to the OSDRs observed in area 1 (Supplementary Fig. S5).

3.4. The transitional domain to the south of the LOC (area 3)

The area 3 (see Fig. 3) to the south of the LOC shows a progressively deeper and rougher top basement reaching >8 s TWTT. Some parts of the top basement still show high reflectivity, but the top basement becomes less reflective continentwards as intense normal faulting results in numerous rotated blocks (see Electronic Supplement 1). These normal faults, mainly dipping oceanwards, are rooting at a discontinuous horizontal reflector at ~1 s TWTT depth beneath the top basement. This reflector has been called UR (for upper reflector) by Gillard et al. (2019) in contrast to a discontinuous weaker lower reflector (LR) that is observed locally deeper at about 10 s TWTT. Some of these normal faults are sealed by horizontal shallow reflectors in the uppermost basement. Deep reflectors are also observed in area 3 (see Figs. 3 and Electronic Supplement 1). Close to the LOC, one of these reflectors is observed dipping continentwards as deep as 11 s TWTT (Fig. 3).

4. Discussion

4.1. Synthesis of observations and first order interpretation away of the LOC

Both the alternating series of ODRs and CDRs and the local crosscutting relationships between these reflectors contrast with earlier observations of lower crustal reflectors dipping predominantly toward the paleo-ridge axis (e.g. Bécel et al., 2015; Ding et al., 2018; Reston et al., 1999). These new observations indicate that the ODRs and CDRs may locally be formed contemporaneously. We describe hereafter, from top to bottom of the oceanic crust, the various reflectors and infer their nature.

We interpret the CDRs that are locally reaching the upper crust as rotated dikes as they are distributed below, perpendicular to the OSDRs that we interpret as lava flows (Fig. 6). This systematic dipping of the shallowest lava flows toward the ridge and the rotation of the sheeted dike complex were described at fast-spreading centers by Karson (2002) on the basis of geological investigations of major fault scarps and DSDP/ODP Drill Holes. Evidence of shallow block rotation pre-dating the cessation of the magmatic activity along ridge parallel normal faults (i.e. with the same orientation as the deep faults) were also reported in Oman (MacLeod and Rothery, 1992).

The flat top basement above the wedges of OSDRs indicates that their formation occurred close enough to the paleo-ridge axis so that the latest lava flows within the neo-volcanic zone at the paleo-ridge axis sealed these wedges that were not deformed subsequently on the ridge flank. The neo-volcanic zone at fast-spreading ridges (zone of lava accumulation and dike intrusion at the ridge axis) is usually very narrow, few kilometers wide but the extent of these wedges within our study area shows that it may reach up to 10 km off-axis.

The rotation of the dikes and lava flows in the uppermost part of the crust must be accommodated below. The apparent sigmoid shape of the CDRs and ODRs and the local occurrence of a horizontal reflector marking the top of the layer of these dipping reflectors suggest a decoupling layer there that could serve both for the CDRs and ODRs in the lower crust and for the rotated dikes above (Figs. 4 and S2). It is located at 0.7-0.8 s TWTT below the top basement (~1.9 km at 5 km/s), which corresponds to the depth of the magma chamber at fast-spreading ridges and therefore to the base of the dike complex. A decoupling level at the base of the dike complex was already suggested by Varga et al. (2004).

At the base of the crust, the rooting of the dipping reflectors onto the Moho indicates that this latter corresponds to another decoupling level (Figs. 3 and 7). The nearly horizontal reflection Moho together with the smooth top basement suggest that the processes forming these dipping reflectors are restricted to the lower crust as neither the base nor the top of the crust are affected. Considering that water is unlikely to penetrate down to 11.5 s TWTT deep within the mantle beneath a relatively thick magmatic crust, we suggest that the local occurrence of dipping reflectors in the mantle (Fig. 5) is best explained at depth by melt intrusions.

4.2. Synthesis of observations and first order interpretation close to the LOC

The dense network of ODRs close to the LOC is not observed elsewhere in the Enderby Basin, suggesting that it is a specific feature at the onset of spreading. The thicker oceanic crust (~0.3 s TWTT more that is ~1 km thicker than normal) closer to the LOC than away shows that the magma supply was up to 15% larger at the onset of spreading than afterwards. This increase of the magma supply was sudden as suggested by the 1 km-high step-up in the top basement above the termination of the reflection Moho. We interpret the pile of shallow reflectors within this step-up as a thick wedge of lavas flowing toward the continent (Supplementary Fig. S5). The base of this wedge could then correspond to the paleo-top basement of a pre-oceanic domain. The loading of volcanic material may have produced the flexure of this existing lithosphere.

The crustal thickness returned normal (2-2.1 s TWTT) after the onset of spreading. It decreased progressively as testified by a flat top basement and a ridgewards rising reflection Moho (see Fig. 3 and Electronic Supplement 1). There, starting from the LOC area, the ODRs become shorter, are progressively replaced by CDRs and finally terminate when the crustal thickness returns to normal. This suggests therefore a control of the occurrence ODRs *vs.* CDRs by the magma supply at the initial ridge.

This magma supply at the initial ridge may also display some variations. We have shown that locally the set of ODRs is replaced by CDRs just beneath a small asymmetric basin at the top basement and a wedge of lava flows underneath (Supplementary Fig. S4), which suggests a syn-tectonic volcanic building and thus a tectonic control. We therefore propose that there is a tradeoff between magma supply and extensional tectonics within the LOC area and that this tradeoff controlled the changes from ODRs to CDRs. For example, a basin at the top basement with a syn-tectonic wedge of lava flows underneath would indicate either less magma supply or a higher extensional rate that controls the termination of the set of ODRs. Alternating triangular-shaped areas with preferentially ODRs or CDRs (Fig. 3) would then show that this tradeoff could change over a short time scale. However, the nearly flat top

basement above these dipping reflectors, shows that the proximity to the ridge axis may allow the equalization of the overall magma supply on a longer time scale by leveling the relief by the latest lava flows. Without well constrained spreading rates for the Enderby Basin, we cannot estimate these time scales.

Close to the LOC, the dense network of deep oceanward dipping reflectors that systematically sole out onto a sharp and highly reflective Moho suggests that the Moho behaved as a decoupling layer. Moreover, the branching out of the reflection Moho at its continentward termination, following either ODRs or CDRs that are also observed in the transitional domain to the south of the LOC (Supplementary Fig. S5), also suggests a tectonic control of the deepest structures of the lower oceanic crust at the onset of spreading. Therefore we propose that, although the initial spreading center can be largely seen as a magmatic system like the EPR (where plate separation is accommodated by ~2% tectonic strain; Escartín et al., 2007) relative to the adjacent hyper-extended and intruded continental lithosphere (Gillard et al., 2019), the newly formed oceanic crust may be deformed. The denser network of dipping reflectors close to the LOC would then suggest that this tectonic deformation is slightly more intense at the onset of spreading than later, once the oceanic ridge is more mature.

The progressively deeper and rougher top basement to the south of the LOC (Fig. 3) was interpreted as exhumed mantle with increasing magmatic addition toward the LOC (Gillard et al., 2019). This is also shown by normal faults that are sealed by lava flows close to the LOC but that offset the top basement far away from it. Such increasing magma volume from the continent toward the ocean with magma addition both on the top and within the basement together with complex magma-fault relationships have already been described in other magma-poor rifted margins (Gillard et al., 2017).

4.3. How do observations in the Oman ophiolite help to understand the nature and the origin of the lower crustal dipping reflectors?

Bécel et al. (2015) proposed that the lower crustal dipping reflections within the fast spread crust offshore Alaska arise from shear zones that form near the spreading center. They extensively discuss the physical properties of tectonic and magmatic features that could ultimately be imaged in the lower oceanic crust. They conclude that either solidified melt that was segregated within the shear structures, mylonitization along shear zones, crystal alignment and/or a combination of these processes may result in the bright dipping reflections (Bécel et al., 2015). These authors noted, however, that shear zones with scales similar to the lower crustal reflections they imaged have not been observed to date in ophiolites, with special reference to the Oman ophiolite supposed to have formed in a similar tectonic setting than their study area. As seen above (section 2.2), this assertion is contradicted by recent observations in Oman that led to revisiting previous interpretations.

Accordingly, we suggest that syn-magmatic normal faulting revealed by new observations in the Oman ophiolite may correspond to the lower crustal dipping reflectors described in this study. We note similarities with the geometry of the dipping reflectors in the oceanic crust. They both dip either ridgeward or continentward within the lower crust and root at the crust-mantle transition zone. They also both occur within the hot ridge axial zone as evidenced by the latest lava flows sealing the top basement that remains almost flat and undeformed. It is important to note that the overall internal

555 deformation is quite variable in Oman, where we observed faults with small normal
556 displacement and major shear zones with displacement reaching likely one or more
557 kilometers. The thickness of these major shear zones may reach tens of meters and
558 could thus be wide enough to be imaged by seismic reflection techniques. In Oman,
559 the faults appear to be closer spaced than on the seismic reflection profiles but this is
560 likely a question of spatial resolution.

561 Following Bécel et al. (2015), we hypothesize that the bright reflections observed in
562 our seismic data set might have a hybrid tectonic and magmatic origin. In Oman, both
563 late magmatic intrusions and low-temperature water circulation occur within the syn-
564 magmatic fault zones. The water introduction produced mineralogical reactions that
565 were active down to greenschist facies and that are absent from gabbroic cumulates
566 located away of the fault zone. We therefore suggest that these lithological
567 modifications, restricted to the vicinity of syn-magmatic fault zones, may result in
568 velocity and density contrasts sufficient enough to create an impedance contrast at the
569 location of these faults. We further speculate that these processes could thus explain
570 the brightness of the dipping reflectors observed in our seismic reflection profiles.
571 Another possible interpretation might be looked for in the anisotropy/polarizing effects
572 related to the igneous layering. Away from faults the bedding is quite regular but this
573 regularity is totally lost in the vicinity (hundreds of meters) of syn-magmatic faults, as
574 illustrated by our observations in Oman. This sudden lack of regularity (which goes
575 along with an increase in alteration) might induce contrasts in the seismic wave
576 propagation and be imaged as a reflector. More work is needed to reinforce the
577 comparison between lower crustal dipping reflectors and syn-magmatic faults.

578 *4.4. Toward a more complex model of magmatic accretion*

579 Summing up our observations of lower crustal dipping reflectors in the Enderby Basin
580 and their comparison with syn-magmatic and high temperature ductile faults observed
581 in the Oman ophiolite suggest that internal sub-axial deformation processes are more
582 complicated than those shown in most current models of mid-ocean ridges. As a matter
583 of fact, one of the main point revealed by studies in the Oman ophiolite is that very high
584 temperature (up to syn-magmatic), high temperature (sub-solidus plastic deformation)
585 and low temperature (brittle) deformation may coexist along the same fault over
586 distances of several hundred meters at Moho depth. This huge temperature gradient
587 likely results from the juxtaposition and interaction between crystallizing magmas and
588 hydrothermal fluids induced by the episodic nucleation of faults in a context of
589 continuous spreading (Rospabé et al., 2019).

590 A clear effect of crustal deformation is the rotation of originally horizontal lava flows
591 and originally steeply dipping dikes to ridgeward and outward-dipping orientations,
592 respectively (Fig. 8). These rotations are evident in outcrops of the upper crust at fast-
593 spreading centers and in the Oman ophiolite (MacLeod and Rothery, 1992; Pallister
594 and Hopson, 1981). Axial loading of lavas is generally considered to be the driving
595 mechanism for this asymmetrical, subsidence of upper crustal units (Dewey and Kidd,
596 1977). This sub-axial subsidence is rapid beneath the ridge axis and decreases up to
597 the edge of the active volcanic zone, a few kilometers for fast-spreading ridges
598 (Karson, 2002). However, our observations show that, within this axial zone,
599 deformation may affect the underlying deeper gabbroic units as well.

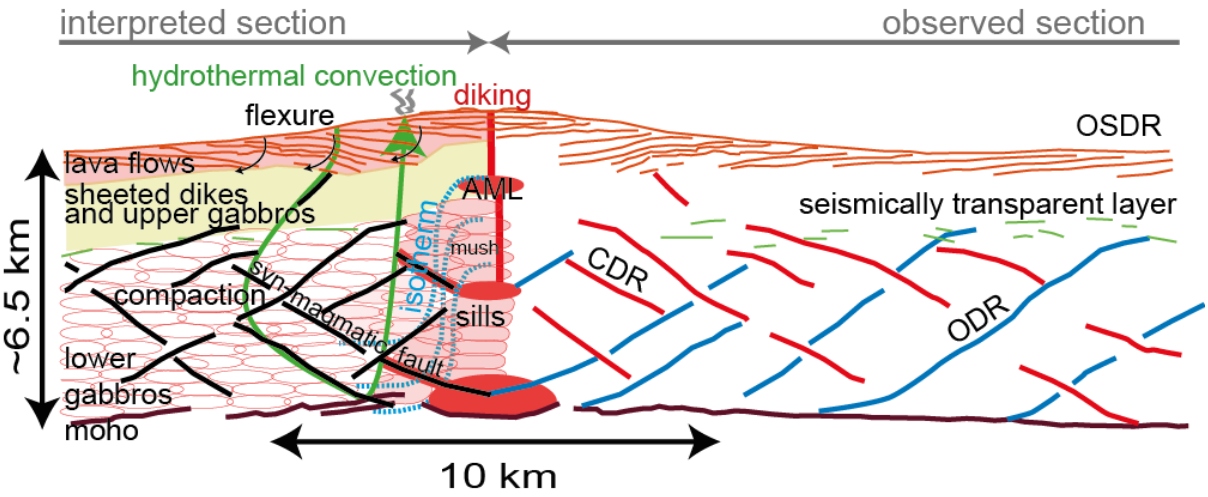

Fig. 8: Cartoon of the structure of the oceanic ridge showing the formation of dipping reflectors by sub-axial deformation (CDR, continentwards dipping reflectors; ODR, oceanwards dipping reflectors; OSDR, oceanic seaward dipping reflectors). Oblique reflectors in the lower crust are syn-magmatic faults. Isotherms (dotted blue lines) and hydrothermal circulation paths (green line) are schematic. AML: axial melt lens. No vertical exaggeration.

Flexure of the upper crustal units in the brittle regime creates accommodation space. At deeper levels, we suggest that early, syn- to sub-magmatic deformation as well as later brittle deformation is accommodated by syn-magmatic faulting as evidenced by the network of the dipping reflectors in the lower oceanic crust (Fig. 8). We infer a decoupling level at the base of the dikes, as already suggested by Karson et al. (2002) and Varga et al. (2004) for the fast-spreading East Pacific Rise, which results in a partitioning of the deformation between the upper and lower crust. Gabbroic sills may have been emplaced beneath the dike complex and not have fully crystallized when the subsidence and deformation occurred in overlying units (Karson et al., 2015; Yoshinobu and Harper, 2004).

Differences in melt supply along the axis of the fast-spreading East Pacific Rise have been mapped by seismic reflection experiments with pure melt zones, inferred to correspond to regions of fresh magma supply from the mantle asthenosphere, and mush zones, inferred to have undergone cooling and crystallization and to be more evolved (Singh et al., 1998). Significant temporal heterogeneities in the magma plumbing system beneath this ridge were also suggested to account for the observed differences between the geochemistry and petrology of the plutonic rocks recovered from Hess Deep and Pito Deep (Perk et al., 2007). We suggest that such short timescale changes of magma supply and subsequent thermal structure may influence the lower crustal sub-axial deformation. The predominance of ODRs in the lower crust during high magma delivery at the onset of seafloor spreading suggests that syn-magmatic faults rooting at the Moho are a particularly efficient way for accommodating space at the base of the crust in the hot axial zone in addition to new melt intrusions (Fig. 8). The occurrence of CDRs on top of the ODRs and their progressive lengthening and deepening up to the complete replacement of the ODRs while the magma supply turns back to normal would then suggest that CDRs rather result from the compaction and subsidence of the lower crust as it cools. This mode of spreading with somewhat less magma supply is more likely to trigger vertical mass transport. Some of the CDRs that reach locally the upper crust may thus indicate an episodic coupling of the upper and lower crust when the magma budget/pressure is lower. Both ODRs and CDRs are thus contemporaneous and participate to the hydrothermal cooling of the crust but their

extent could be related to the tradeoff between magma supply and tectonic deformation. This latter is probably relatively constant at the mature spreading center but may be variable at the onset of spreading.

5. Conclusions

The main results of our interpretation of high-quality seismic reflection profiles across the ocean-continent transition in the Enderby Basin, between the Kerguelen Plateau and the Antarctic margin, are as follows:

1. While lower crustal events dipping toward the paleo-ridge axis were predominantly described until now, we identified numerous both ridgeward and continentward dipping high-amplitude dipping reflectors in the lower oceanic crust;
2. We suggest that these lower crustal dipping reflectors correspond to syn-magmatic faults previously described in the Oman ophiolite;
3. Evidence for such syn-accretion tectonism at depth together with the systematic rotation of originally horizontal lava flows pre-dating the cessation of the magmatic activity argue for deformation within the axial zone of magmatic spreading centers.

Acknowledgements

Seismic sections of the AGSO surveys GA-228 and GA-229 have been provided by Geoscience Australia and are published with the permission of Geoscience Australia. These seismic data are freely available from Geoscience Australia upon request. We would like to acknowledge the support and kindness of Aaron Rockey and the other employees of Geoscience Australia. Gravity grid of Sandwell et al. (2014) is freely available from the website of the UCSD (topex.ucsd.edu/cgi-bin/get_data.cgi). We thank Alexander Golynsky for providing the magnetic grid of the Antarctic margin. We also gratefully acknowledge Jeffrey Karson and the Editor, Jean-Philippe Avouac, for their review and helpful comments. Support was provided by the French Institut National des Sciences de l'Univers INSU-CNRS.

Figure captions:

Fig. 1: Map of the eastern Enderby Basin. The background image is the free air gravity anomaly grid derived from satellite altimetry data (Sandwell et al., 2014). The black dashed line indicates the landward edge of the oceanic crust (LOC) after Gaina et al. (2007). The white dashed line indicates the presumed extinct ridge axis after Gibbons et al. (2013). The squares show the magnetic anomaly picks from Gibbons et al. (2013). The black lines indicate the seismic profiles from Geoscience Australia used in this paper. Their thickened and dashed parts correspond to the sections shown in Fig. 3. The white star indicates the location of Fig. 6. Ker., Kerguelen Island; CIR, Central Indian Ridge; SEIR, Southeast Indian Ridge; SWIR, Southwest Indian Ridge.

Fig. 2: Evidence of syn-magmatic normal faulting and block rotation at Moho level in the Oman ophiolite, Maqsad area (see also Abily et al. (2011)). (a) Simplistic sketches

illustrating the possible context of acquisition of the structures observed in the field (left) and the evolution in the conditions of deformation along the fault (right). (b) Main structural elements observed on this outcrop: magmatic layering (thin black lines); ductile faults (thick black lines and arrows), deformed crystal mush layer (red symbols). (c) Closer view on the zone of former crystal mush with complex modal layering induced by crystal sorting and melt injection during viscous deformation. (d) Detail on a ptygmatic fold and on the upper horizon of pegmatite (former melt layer that made possible the mechanical decoupling between the tilted blocks of layered cumulates and the overlying cumulates).

Fig. 3: Line drawing of 4 seismic profiles across the landward edge of the oceanic crust (LOC indicated by the green band). Blue lines indicate oceanward dipping reflectors (ODRs); red ones indicate continentward dipping reflectors (CDRs); yellow ones show nearly horizontal reflectors and orange ones at the top basement indicate oceanic seawards dipping reflectors (OSDRs). The thick orange lines at the bottom of the crust show the reflection Moho and the black lines beneath it show where the Moho is continuous and highly reflective. The blue band indicates the ridgeward end of the dense network of ODRs occurring close to the LOC. Vertical exaggeration is approximately x2. Uninterpreted and interpreted versions of profiles 229/32 with no vertical exaggeration are shown in the Electronic Supplement 1.

Fig. 4: Examples of dipping reflectors crossing each other (a: profile 229/32 and b: profile 228/07) defining a layer of almost constant thickness at the base of the oceanic crust. The reflection Moho is well marked almost all along the bottom of the layer. See figure caption and location in Fig. 3. Approximately no vertical exaggeration. Copyright Commonwealth of Australia (Geoscience Australia).

Fig. 5: Example of reflectors that are observed both in the crust and in the mantle as deep as 11.5 s TWTT (line 229/33). Note some rare examples of dipping reflectors that are shallowing but do not reach the top basement as they are covered by long and continuous reflectors. See figure caption and location in Fig. 3. Approximately no vertical exaggeration. Copyright Commonwealth of Australia (Geoscience Australia).

Fig. 6: Example of oceanic seawards dipping reflectors (OSDRs) forming up to ~10 km-long wedges in the uppermost part of the crust (profile 229/31). Same figure caption as Fig. 3. See location in Fig. 1. Approximately no vertical exaggeration. Copyright Commonwealth of Australia (Geoscience Australia).

Fig. 7: Denser network of oceanward dipping reflectors (ODRs) and continentward dipping reflectors (CDRs) (1 reflector every ~500 m) close to the landward edge of the oceanic crust (profile 229/32). Vertical exaggeration is approximately 2x. See figure caption and location in Fig. 3. Copyright Commonwealth of Australia (Geoscience Australia).

Fig. 8: Cartoon of the structure of the oceanic ridge showing the formation of dipping reflectors by sub-axial deformation (CDR, continentwards dipping reflectors; ODR, oceanwards dipping reflectors; OSDR, oceanic seaward dipping reflectors). Oblique reflectors in the lower crust are syn-magmatic faults. Isotherms (dotted blue lines) and hydrothermal circulation paths (green line) are schematic. AML: axial melt lens. No vertical exaggeration.

REFERENCES CITED

Abily, B., Ceuleneer, G., and Launeau, P., 2011, Synmagmatic normal faulting in the lower oceanic crust: Evidence from the Oman ophiolite: Geology, v. 39, p. 391-394, doi:10.1130/g31652.1.

Amri, I., Benoit, M., and Ceulenner, G., 1996, Tectonic setting for the genesis of oceanic plagiogranites: evidence from a paleo-spreading structure in the Oman ophiolite: Earth and Planetary Science Letters, v. 139, p. 177-194.

Bécel, A., Shillington, D.J., Nedimović, M.R., Webb, S.C., and Kuehn, H., 2015, Origin of dipping structures in fast-spreading oceanic lower crust offshore Alaska imaged by multichannel seismic data: Earth and Planetary Science Letters, v. 424, p. 26-37, doi:http://dx.doi.org/10.1016/j.epsl.2015.05.016.

Boudier, F., Bouchez, J.-L., Nicolas, A., Cannat, M., Ceuleneer, G., Misseri, M., and Montigny, R., 1985, Kinematics of oceanic thrusting in the Oman ophiolite: model of plate convergence: Earth and Planetary Science Letters, v. 75, p. 215-222.

Boudier, F., Ceuleneer, G., and Nicolas, A., 1988, Shear zones, thrusts and related magmatism in the Oman ophiolite: Initiation of thrusting on an oceanic ridge: Tectonophysics, v. 151, p. 275-296, doi:https://doi.org/10.1016/0040-1951(88)90249-1.

Brown, T.C., Cheadle, M.J., John, B.E., Coogan, L.A., Gee, J.S., Karson, J.A., and Swapp, S.M., 2019, Textural Character of Gabbroic Rocks from Pito Deep: a Record of Magmatic Processes and the Genesis of the Upper Plutonic Crust at Fast-Spreading Mid-Ocean Ridges: Journal of Petrology, v. 60, p. 997-1026, doi:10.1093/petrology/egz022.

Canales, J.P., Detrick, R.S., Toomey, D.R., and Wilcock, S.D., 2003, Segment-scale variations in crustal structure of 150- to 300-k.y.-Old fast spreading oceanic crust (East Pacific Rise, 8°15'N-10°15'N from wide-angle seismic refraction profiles: Geophysical Journal International, v. 152, p. 766-794.

Ceuleneer, G., Abily, B., Python, M., Kaczmarek, M.-A., Rospabé, M., Grégoire, M., Benoit, M., and le Sueur, E., 2020, Crustal accretion along a giant high-temperature normal fault at the front of the Oman ophiolite: evidence from the Bahla and some other massifs, International Conference on Ophiolites and the Oceanic Lithosphere: Results of the Oman Drilling Project and Related Research: Muscat, Sultanate of Oman, Sultan Qaboos University, p. 3.

Ceuleneer, G., Monnereau, M., and Amri, I., 1996, Thermal structure of a fossil mantle diapir inferred from the distribution of mafic cumulates: Nature, v. 379, p. 149-153, doi:10.1038/379149a0.

Christeson, G.L., Goff, J.A., and Reece, R.S., 2019, Synthesis of Oceanic Crustal Structure from Two-Dimensional Seismic Profiles: Reviews of Geophysics, v. 57, p. 504-529, doi:10.1029/2019rg000641.

761 Collins, J.A., Brocher, T.M., and Karson, J.A., 1986, Two-dimensional seismic
762 reflection modeling of the inferred fossil oceanic crust/mantle transition in the
763 Bay of Islands Ophiolite: Journal of Geophysical Research: Solid Earth, v. 91,
764 p. 12520-12538, doi:10.1029/JB091iB12p12520.

765 Constantin, M., Hékinian, R., Bideau, D., and Hébert, R.j., 1996, Construction of the
766 oceanic lithosphere by magmatic intrusions: Petrological evidence from
767 plutonic rocks formed along the fast-spreading East Pacific Rise: Geology, v.
768 24, p. 731-734, doi:10.1130/0091-7613(1996)024<0731:cotolb>2.3.co;2.

769 Crawford, W.C., and Webb, S.C., 2002, Variations in the distribution of magma in the
770 lower crust and at the Moho beneath the East Pacific Rise at 9°-10°N: Earth
771 and Planetary Science Letters, v. 202, p. 117-130.

772 Davis, J.K., Lawver, L.A., Norton, I.O., Dalziel, I.W.D., and Gahagan, L.M., 2018, The
773 crustal structure of the Enderby Basin, East Antarctica: Marine Geophysical
774 Research, v. 40, p. 1-16, doi:10.1007/s11001-018-9356-5.

775 Detrick, R.S., Buhl, P., Vera, E.E., Mutter, J.C., Orcutt, J.A., Madsen, J.A., and
776 Brocher, T.M., 1987, Multi-channel seismic imaging of a crustal magma
777 chamber along the East Pacific Rise: Nature, v. 326, p. 35-41.

778 Dewey, J.F., and Kidd, W.S.F., 1977, Geometry of plate accretion: GSA Bulletin, v. 88,
779 p. 960-968, doi:10.1130/0016-7606(1977)88<960:gopa>2.0.co;2.

780 Dijkstra, A.H., Drury, M.R., and Frijhoff, R.M., 2002, Microstructures and lattices in the
781 Hilti mantle section (Oman Ophiolite): Evidence for shear localization and melt
782 weakening in the crust mantle transition zone?: Journal of Geophysical
783 Research, v. 107, p. 10.1029/2001JB000458.

784 Ding, W., Sun, Z., Dadd, K., Fang, Y., and Li, J., 2018, Structures within the oceanic
785 crust of the central South China Sea basin and their implications for oceanic
786 accretionary processes: Earth and Planetary Science Letters, v. 488, p. 115-
787 125, doi:https://doi.org/10.1016/j.epsl.2018.02.011.

788 Escartín, J., Soule, S.A., Fornari, D.J., Tivey, M.A., Schouten, H., and Perfit, M.R.,
789 2007, Interplay between faults and lava flows in construction of the upper
790 oceanic crust: The East Pacific Rise crest 9°25′–9°58′N: Geochemistry,
791 Geophysics, Geosystems, v. 8, doi:10.1029/2006gc001399.

792 Gaina, C., Muller, R.D., Brown, B., Ishihara, T., and Ivanov, S., 2007, Breakup and
793 early seafloor spreading between India and Antarctica: Geophysical Journal
794 International, v. 170, p. 151-169, doi:doi:10.1111/j.1365-246X.2007.03450.x.

795 Gibbons, A.D., Whittaker, J.M., and Müller, R.D., 2013, The breakup of East
796 Gondwana: Assimilating constraints from Cretaceous ocean basins around
797 India into a best-fit tectonic model: Journal of Geophysical Research: Solid
798 Earth, v. 118, p. 808-822, doi:10.1002/jgrb.50079.

799 Gillard, M., Sauter, D., Tugend, J., Tomasi, S., Epin, M.-E., and Manatschal, G., 2017,
800 Birth of an oceanic spreading center at a magma-poor rift system: Scientific
801 Reports, v. 7, p. 15072, doi:10.1038/s41598-017-15522-2.

802 Gillard, M., Tugend, J., Müntener, O., Manatschal, G., Karner, G.D., Autin, J., Sauter,
803 D., Figueredo, P.H., and Ulrich, M., 2019, The role of serpentinization and
804 magmatism in the formation of decoupling interfaces at magma-poor rifted
805 margins: Earth-Science Reviews, v. 196, p. 102882,
806 doi:https://doi.org/10.1016/j.earscirev.2019.102882.

807 Gillis, K.M., Snow, J.E., Klaus, A., Abe, N., Adriao, A.B., Akizawa, N., Ceuleneer, G.,
808 Cheadle, M.J., Faak, K., Falloon, T.J., Friedman, S.A., Godard, M., Guerin, G.,
809 Harigane, Y., Horst, A.J., Hoshide, T., Ildefonse, B., Jean, M.M., John, B.E.,
810 Koepke, J., Machi, S., Maeda, J., Marks, N.E., McCaig, A.M., Meyer, R.,
811 Morris, A., Nozaka, T., Python, M., Saha, A., and Wintsch, R.P., 2014,
812 Primitive layered gabbros from fast-spreading lower oceanic crust: Nature, v.
813 505, p. 204-207, doi:10.1038/nature12778.

814 Golynsky, A.V., Ivanov, S.V., Kazankov, A.J., Jokat, W., Masolov, V.N., and von Frese,
815 R.R.B., 2013, New continental margin magnetic anomalies of East Antarctica:
816 Tectonophysics, v. 585, p. 172-184,
817 doi:http://dx.doi.org/10.1016/j.tecto.2012.06.043.

818 Jokat, W., Nogi, Y., and Leinweber, V., 2010, New aeromagnetic data from the western
819 Enderby Basin and consequences for Antarctic-India break-up: Geophysical
820 Research Letters, v. 37, p. L21311, doi:10.1029/2010gl045117.

821 Jousselin, D., and Nicolas, A., 2000, The Moho transition in the Oman ophiolite -
822 relation with wherlites in the crust and dunites in the mantle: Marine
823 Geophysical Researches, v. 21, p. 229-241.

824 Jousselin, D., Nicolas, A., and Boudier, F., 1998, Detailed mapping of a mantle diapir
825 below a paleo-spreading center in the Oman ophiolite: Journal of Geophysical
826 Research: Solid Earth, v. 103, p. 18153-18170, doi:10.1029/98jb01493.

827 Karson, J.A., 2002, Geologic Structure of uppermost oceanic crust created at fast to
828 intermediate-rate spreading centers: Annual Reviews of Earth and Planetary
829 Sciences, v. 30, p. 10.1146/annurev.earth.30.091201.141132.

830 Karson, J.A., Kelley, D.S., Fornari, D.J., Perfit, M.R., and Shank, T.M., 2015,
831 Discovering the Deep: A Photographic Atlas of the Seafloor and Ocean Crust,
832 Cambridge University Press, 413 p.

833 Karson, J.A., Klein, E.M., Hurst, S.D., Lee, C.D., Rivizzigno, P.A., Curewitz, D., Morris,
834 A.R., and Party, H.D.S., 2002, Structure of uppermost fast-spreading oceanic
835 crust exposed at the Hess Deep Rift: Implications for subaxial processes at
836 the East Pacific Rise: Geochemistry, Geophysics, Geosystems, v. 3, p.
837 2001GC000155.

838 Kelemen, P.B., Koga, K., and Shimizu, N., 1997, Geochemistry of gabbro sills in the
839 crust/mantle transition zone of the Oman ophiolite: Implications for the origin
840 of the oceanic lower crust: Earth and Planetary Science Letters, v. 146, p. 475-
841 488.

842 MacLeod, C.J., Johan Lissenberg, C., and Bibby, L.E., 2013, “Moist MORB” axial
843 magmatism in the Oman ophiolite: The evidence against a mid-ocean ridge
844 origin: Geology, v. 41, p. 459-462, doi:10.1130/g33904.1.

845 MacLeod, C.J., and Rothery, D.A., 1992, Ridge axial segmentation in the Oman
846 ophiolite: evidence from along-strike variations in the sheeted dyke complex,
847 in Parson, L.M., Murton, B.J., and Browning, P., eds., Ophiolites and their
848 modern oceanic analogues, Volume 60: Geological Society Special
849 Publication, Geological Society, p. 39-63.

850 MacLeod, S.J., Williams, S.E., Matthews, K.J., Müller, R.D., and Qin, X., 2017, A global
851 review and digital database of large-scale extinct spreading centers:
852 Geosphere, v. 13, p. 911-949, doi:10.1130/ges01379.1.

853 Marjanovic, M., Carbotte, S.M., Carton, H., Nedimovic, M.R., Mutter, J.C., and
854 Canales, J.P., 2014, A multi-sill magma plumbing system beneath the axis of
855 the East Pacific Rise: Nature Geosci, v. 7, p. 825-829, doi:10.1038/ngeo2272.

856 McElhinny, M.W., 1970, Formation of the Indian Ocean: Nature, v. 228, p. 977-979,
857 doi:10.1038/228977a0.

858 Nicolas, A., and Boudier, F., 2015, Structural contribution from the Oman ophiolite to
859 processes of crustal accretion at the East Pacific Rise: Terra Nova, v. 27, p.
860 77-96, doi:10.1111/ter.12137.

861 Pallister, J.S., and Hopson, C., 1981, Samail Ophiolite plutonic suite: Field relations,
862 phase variation, cryptic variation and layering, and a model of a spreading
863 ridge magma chamber: Journal of Geophysical Research, v. 86, p. 2593-2644.

864 Perk, N.W., Coogan, L.A., Karson, J.A., Klein, E.M., and Hanna, H.D., 2007, Petrology
865 and geochemistry of primitive lower oceanic crust from Pito Deep: implications
866 for the accretion of the lower crust at the Southern East Pacific Rise:
867 Contributions to Mineralogy and Petrology, v. 154, p. 575-590,
868 doi:10.1007/s00410-007-0210-z.

869 Quick, J.E., and Delinger, R.P., 1993, Ductile deformation and the origin of layered
870 gabbro in ophiolites: Journal of Geophysical Research, v. 98, p. 14015-14027.

871 Reston, T.J., Ranero, C.R., and Belykh, I., 1999, The structure of Cretaceous oceanic
872 crust of the NW Pacific: Constraints on processes at fast spreading centers:
873 Journal of Geophysical Research: Solid Earth, v. 104, p. 629-644,
874 doi:10.1029/98jb02640.

875 Rioux, M., Bowring, S., Kelemen, P., Gordon, S., Dudás, F., and Miller, R., 2012, Rapid
876 crustal accretion and magma assimilation in the Oman-U.A.E. ophiolite: High

precision U-Pb zircon geochronology of the gabbroic crust: Journal of Geophysical Research: Solid Earth, v. 117, doi:10.1029/2012jb009273.

Rospabé, M., Benoit, M., Ceuleneer, G., Kaczmarek, M.-A., and Hodel, F., 2019, Melt hybridization and metasomatism triggered by syn-magmatic faults within the Oman ophiolite: A clue to understand the genesis of the dunitic mantle-crust transition zone: Earth and Planetary Science Letters, v. 516, p. 108-121, doi:https://doi.org/10.1016/j.epsl.2019.04.004.

Rospabé, M., Ceuleneer, G., Benoit, M., Abily, B., and Pinet, P., 2017, Origin of the dunitic mantle-crust transition zone in the Oman ophiolite: The interplay between percolating magmas and high-temperature hydrous fluids: Geology, v. 45, p. 471-474, doi:10.1130/g38778.1.

Sandwell, D.T., Müller, R.D., Smith, W.H.F., Garcia, E., and Francis, R., 2014, New global marine gravity model from CryoSat-2 and Jason-1 reveals buried tectonic structure: Science, v. 346, p. 65-67, doi:10.1126/science.1258213.

Singh, S.C., Kent, G.M., Collier, J.S., Harding, A.J., and Orcutt, J.O., 1998, Melt to mush variations in crustal magma properties along the ridge crest at the southern East Pacific Rise: Nature, v. 394, p. 874-878.

Sinton, J.M., and Dietrick, R.S., 1992, Mid-ocean Ridge magma chambers: J. Geophys. Res., v. 97, p. 197-216.

Stagg, H.M.J., Colwel, J.B., Direen, N.G., O'Brien, P.E., Bernardel, G., Borissova, I., Brown, B.J., and Ishirara, T., 2005, Geology of the Continental Margin of Enderby and Mac. Robertson Lands, East Antarctica: Insights from a Regional Data Set: Marine Geophysical Researches, v. 25, p. 183-219, doi:10.1007/s11001-005-1316-1.

Toomey, D.R., Purdy, G.M., Solomon, S.C., and Wilcock, W.S.D., 1990, The three-dimensional seismic velocity structure of the East Pacific Rise near latitude 9°30' N: Nature, v. 347, p. p. 639-645.

Varga, R.J., Karson, J.A., and Gee, J.S., 2004, Paleomagnetic constraints on deformation models for uppermost oceanic crust exposed at the Hess Deep Rift: Implications for axial processes at the East Pacific Rise: Journal of Geophysical Research: Solid Earth, v. 109, doi:doi:10.1029/2003JB002486.

Yoshinobu, A.S., and Harper, G.D., 2004, Hypersolidus deformation in the lower crust of the Josephine ophiolite: evidence for kinematic decoupling between the upper and lower oceanic crust: Journal of Structural Geology, v. 26, p. 163-175.

Zihlmann, B., Müller, S., Coggon, R.M., Koepke, J., Garbe-Schönberg, D., and Teagle, D.A.H., 2018, Hydrothermal fault zones in the lower oceanic crust: An example from Wadi Gideah, Samail ophiolite, Oman: Lithos, v. 323, p. 103-124, doi:https://doi.org/10.1016/j.lithos.2018.09.008.

916